Influence of the dopant penetration depth on the solar cell performance of n-type interdigitated back contact silicon solar cells

Alexander Korovin, J Alvarez, Jean-Paul Kleider

Available online at www.sciencedirect.com

ScienceDirect

Energy Procedia 92 (2016) 103 – 108

Energy Procedia

6th International Conference on Silicon Photovoltaics, SiliconPV 2016

Influence of the dopant penetration depth on the solar cell performance of *n*-type interdigitated back contact silicon solar cells

Alexander V. Korovin[a,b]*, José Alvarez[a] and Jean-Paul Kleider[a]

[a]*GeePs, UMR CNRS 8507, CentraSupélec, Univ. Paris-Sud, Université Paris-Saclay, Sorbonne Universités UPMC Univ. Paris 6, 3 & 11 rue Joliot Curie, Plateau de Moulon – 91192 Gif sur Yvette, France*
[b]*Institute for Physics of Semiconductors, National Academy of Sciences of Ukraine, 45 Nauky Prospect, Kyiv 03028, Ukraine*

Abstract

In this report a 2D modeling of *n*-type interdigitated back contact (IBC) crystalline silicon (c-Si) solar cell structures is presented for two different types of the BSF and emitter junctions: homojunction cells (referred as IBC-HOMO) and cells combining a homojunction and a heterojunction with hydrogenated amorphous silicon (a-Si:H), also called "hybrid" cells (referred as hybrid IBC). Both structures were analyzed and in particular we studied the effect of doping (peak concentration and penetration depth of the dopants) on the solar cell performances. For doping levels in the range 10^{18}-10^{20} cm^{-3} relatively large dopant penetration depth (>100 nm) demonstrates better solar cell performance in contrary to very shallow penetration depths (10 nm). The best solar cell performance (25.6% conversion efficiency, 740 mV open circuit voltage, 41 mA/cm^2 short circuit current and 84.2% fill factor) were found for hybrid IBC structures involving a BSF heterojunction and a highly doped emitter homojunction ($N_E = 10^{21}$ cm^{-3}) with a dopant penetration depth of 10 nm in the case of *n*-type silicon wafer with a thickness of 100 μm. The implementation of defects at the c-Si/a-Si:H interface in the range (1-5)×10^{11} cm^{-2} shows that hybrid cells with BSF heterojunctions are more affected than the structures with emitter heterojunctions. However, solar cell efficiencies of 25% can be simulated for hybrid cells if the width of the BSF is reduced with respect to the emitter and combined with highly doped homojunctions and shallow dopant penetration depths.

Peer review by the scientific conference committee of SiliconPV 2016 under responsibility of PSE AG.

Keywords: crystalline silicon PV; hydrogenated amorphous silicon PV; back contacts; modeling

* Corresponding author. Tel.: + 33 (0)1 69 85 16 43; fax: +33 (0)1 69 41 83 18.
E-mail address: alexander.korovin@lgep.supelec.fr

Peer review by the scientific conference committee of SiliconPV 2016 under responsibility of PSE AG.
doi:10.1016/j.egypro.2016.07.036

1. Introduction

Interdigitated Back Contact (IBC) silicon solar cells are attractive high efficiency structures that present the advantage of no front grid shadowing and open new opportunities for module interconnection. Sunpower has recently demonstrated 25% efficiency in IBC with homojunction cells (IBC-HOMO) using a standard IBC sequence with 145 μm thick *n*-type CZ Si wafers [1]. Furthermore, the combination of crystalline silicon and hydrogenated amorphous silicon (c-Si/a-Si:H) to produce heterojunctions (HET) in IBC concepts has also been developed by several research groups because of their high efficiency potential (25.6%, Panasonic's world record) with low temperature fabrication process (≤200°C) [1-4]. A mix of both technologies, so called Hybrid IBC cells, offers also an interesting approach to reach high efficiencies by reducing, for example, the resistive losses in IBC-HET. Notably, ion implantation technology shows the capabilities to precisely control the dopant doses (even at the very near-surface) and profiles and appears as a promising way to greatly simplify the fabrication sequence of IBC silicon solar cells which currently requires multiple diffusion steps based on masking and furnace annealing.

On this basis, we focus our study on high efficiency *n*-type silicon IBC structures, namely IBC-HOMO and Hybrid IBC, with the purpose to investigate how the solar cells performances are impacted by the dopant penetration depth and concentration in the precise case of p^+-*n* and/or n^+-*n* homojunctions.

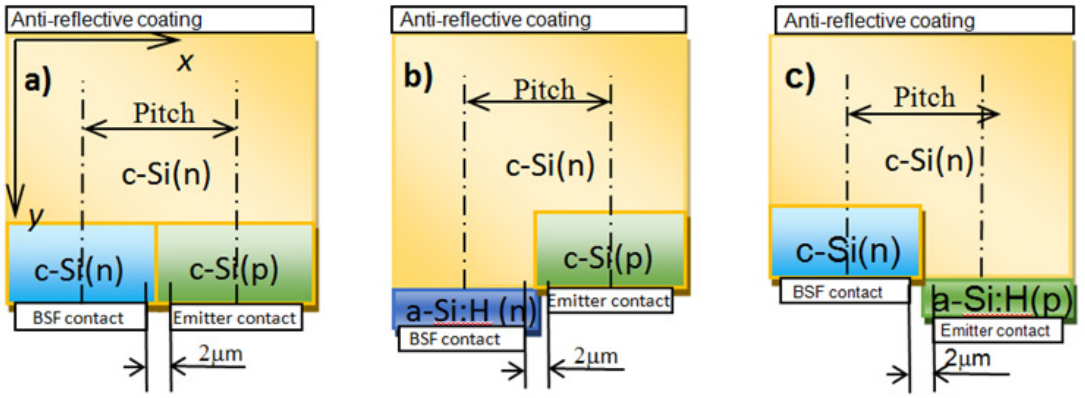

Fig. 1. Schematic cross-sections of *n*-type IBC silicon cell structures: a) homojunctions (IBC-HOMO), hybrid IBC: b) emitter – homojunction/ BSF – heterojunction (HOMO-E/HET-BSF) and c) BSF – homojunction/ emitter – heterojunction (HOMO-BSF/HET-E).

2. Solar cell structures and simulation parameters

The structures under consideration are illustrated in Fig. 1 and consist of *n*-type crystalline silicon wafer with a resistivity of 4.58 Ω·cm and a thickness of 100 µm. For the hybrid cells, two structures are considered according to which one of the emitter or the BSF is the homojunction. The pitch of the structure is 300 µm and the gap between contacts is assumed to be 2 µm. The front surface of the IBC structure is based on an anti-reflective layer with a thickness of 75 nm and a refractive index of 2.05.

The current-voltage characteristics have been simulated using the 2D ATLAS software [5] from Silvaco under illumination of AM1.5 solar light. In our simulations, we took into account the band gap narrowing model, Auger recombination with standard parameters and Shockley-Read-Hall recombination with both electron and hole lifetimes equal to 30 ms, thermionic and tunnel models. The electrons and holes surface recombination velocity are fixed to 7 cm/s at interfaces between semiconductors and insulators taking into account the surface passivation. The influence of a micro-scaled texturization of IBC interfaces was estimated phenomenologically using an average photogeneration rate $G(y) = G_0(y)(1+\gamma)$, where $G_0(y)$ is the photogeneration rate for the multilayer planar structure integrated over the AM1.5 solar spectrum, γ is the phenomenological parameter. We use $\gamma = 0.133$ since it allows us to reproduce the short circuit current density obtained by Panasonic for IBC-HETs for a 150 µm thick 1 Ω·cm *n*-

type wafer [4]. Typical boron (the emitter) or phosphorus (the BSF) profiles show a peak dopant concentration in the range 10^{19}-10^{21} cm^{-3} with a penetration depth in the range 10-1000 nm depending on the doping technological process (thermal diffusion or ion implantation) [6-8]. To describe the dopant profile a Gaussian function, $N(y)$, is implemented: $N(y) = N_{peak}\, e^{-(y-y_0)^2/\delta^2}$, where y_0 is the position of the rear interface, N_{peak} is the peak dopant concentration, δ is the dopant penetration depth. In the presented simulations, the dopant peak concentration is varied from 10^{18} to 10^{21} cm^{-3}. The lateral dopant penetration depth is a quarter of δ. In the case of heterojunctions, the emitter (or BSF) is formed by a 10 nm-thick layer of *p*- (or *n*-) doped amorphous silicon (a-Si:H). The density of states (DOS) in a-Si:H layers is defined by a combination of two exponentially decaying band tail states and two Gaussian distributions of deep defect states. The DOS and doping concentrations were adjusted to set the Fermi level at room temperature at 0.2 eV below the conduction band edge in *n*-type a-Si:H (BSF) and at 0.3 eV above the valence band edge in *p*-type a-Si:H (emitter), values corresponding to experimental data of the activation energies of the dark conductivity in these layers [9]. The gap in amorphous silicon and electron affinity are set to 1.7 eV and 3.87 eV, respectively.

3. Simulation results

The calculated solar cell performances (short circuit current density, J_{SC}, open circuit voltage, V_{OC}, conversion efficiency, *CE*, and fill factor, *FF*) as functions of δ are presented in Fig. 2. For the IBC under consideration the peak dopant concentration of the emitter and/or BSF is fixed at 10^{21} cm^{-3} (N_E, N_{BSF}) and the ratio between the width of the BSF and the period ($R_{BSF/Period}$) is set equal to 0.1. For the IBC-HOMO structures two cases are analyzed specifically when the dopant penetration depth at the BSF is kept constant (δ_{BSF} = 100 nm) and that at the emitter varies, and inversely. Solid and dashed lines represent the parameters J_{SC} and V_{OC} in Fig. 2a or *CE* and *FF* in Fig. 2b, respectively. As it can be seen in Fig. 2b, all the IBC solar cell performances increase for δ below 100 nm, and particularly that of the hybrid IBC cells. The HOMO-E/HET-BSF cell exhibits remarkable performance for δ = 10 nm namely *CE* of 25.6%, *FF* of 84.2%, V_{OC} over 740 mV and J_{SC} close to 41 mA/cm^2.

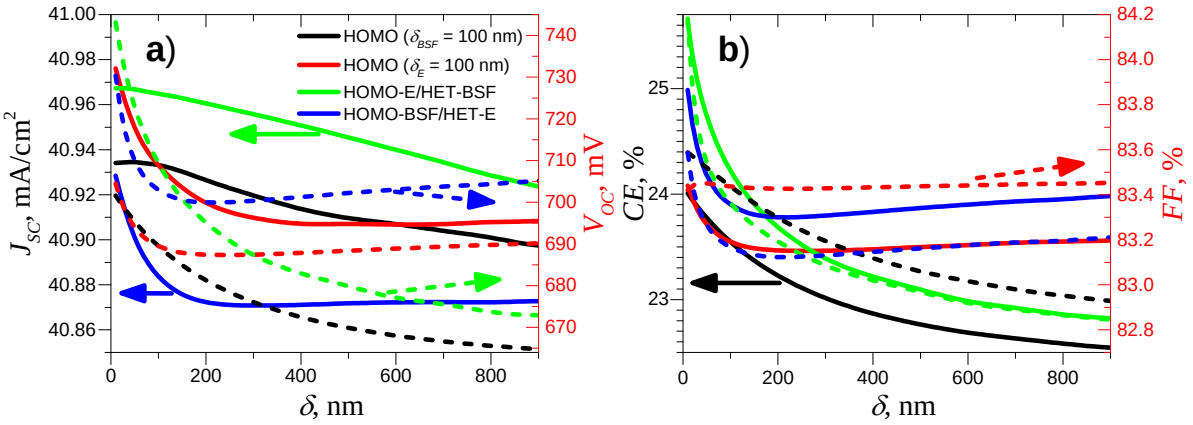

Fig. 2. Calculated solar cell performances: a) short-circuit current density (solid lines) and open circuit voltage (dashed lines), b) conversion efficiency (solid lines) and fill factor (dashed lines), as a function of dopant penetration depth, δ. The peak dopant concentration at the emitter and the BSF is equal to 10^{21} cm^{-3}.

Figure 3 displays the solar cell efficiencies calculated for IBC-HOMO and Hybrid IBC structures as a function of the peak dopant concentration of the emitter, N_E (Fig. 3a,c), or the BSF, N_{BSF} (Fig. 3b,d), and for different values of $R_{BSF/Period}$ and dopant penetration depths (δ = 10 nm and δ = 100 nm). The calculated curves point out a peak dopant threshold (around 10^{20} cm^{-3}) below which a δ = 100 nm associated with a large hetero BSF (case of the HOMO-E/HET-BSF structure with a $R_{BSF/Period}$ = 0.9) or a large hetero emitter (case of the HOMO-BSF/HET-E structure with a $R_{BSF/Period}$ = 0.1) is preferable for efficiency values over 20%. For the case of IBC-HOMO structures a large

emitter ($R_{BSF/Period}$ = 0.1) appears more advantageous. In Fig. 4, the cell efficiencies of Hybrid IBC structures were analysed implementing interface defects at the c-Si/a-Si:H heterojunction. The conversion efficiency was plotted for two different dopant penetration depths (δ = 10 nm (Fig. 4a) and δ = 100 nm (Fig. 4b)) and as a function of $R_{BSF/Period}$. The peak dopant concentration at the emitter or BSF was fixed at 10^{21} cm^{-3}. For the particular case of the HOMO-E/HET-BSF IBC structures a defect density at the interface of 10^{11} cm^{-2} impacts the conversion efficiency for large values of $R_{BSF/Period}$, namely when the HET-BSF width becomes predominant against the HOMO-E. The reduction in *CE* becomes considerable when the defect density is increased to the value of 5×10^{11} cm^{-2}. However, keeping $R_{BSF/Period}$ as low as possible minimizes the *CE* losses: the decrease of *CE* is only 0.6/0.2% (absolute values) for $R_{BSF/Period}$ = 0.1 and δ = 10/100 nm. The HOMO-BSF/HET-E structure seems not impacted by the interface defects, the highest *CE*s being achieved for large HET-E and small HOMO-BSF ($R_{BSF/Period}$ = 0.1).

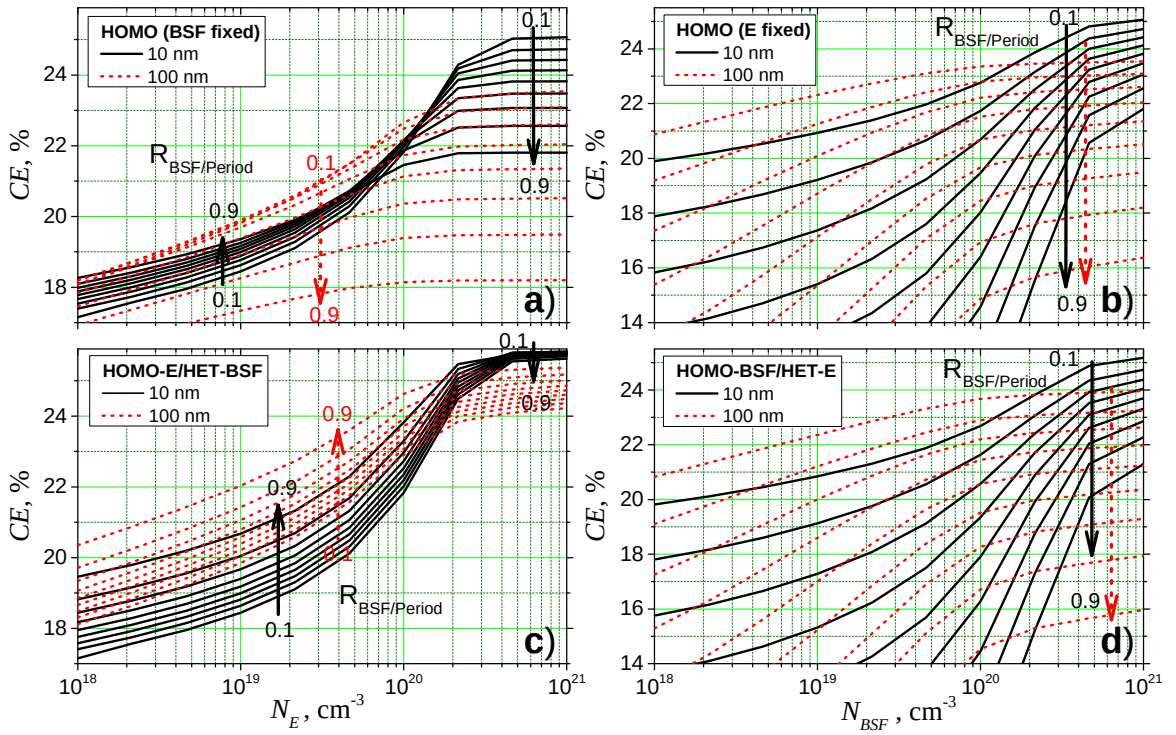

Fig. 3. Conversion efficiency calculated for various types of solar cells, IBC-HOMO (a,b), hybrid IBC, HOMO-E/HET-BSF (c) and HOMO-BSF/HET-E (d), as a function of the peak dopant concentration at the emitter, N_E (a,c), or the BSF, N_{BSF} (b,d), and for different $R_{BSF/Period}$ values. Solid black and dashed red lines correspond to a penetration depth (δ) of 10 nm and 100 nm, respectively.

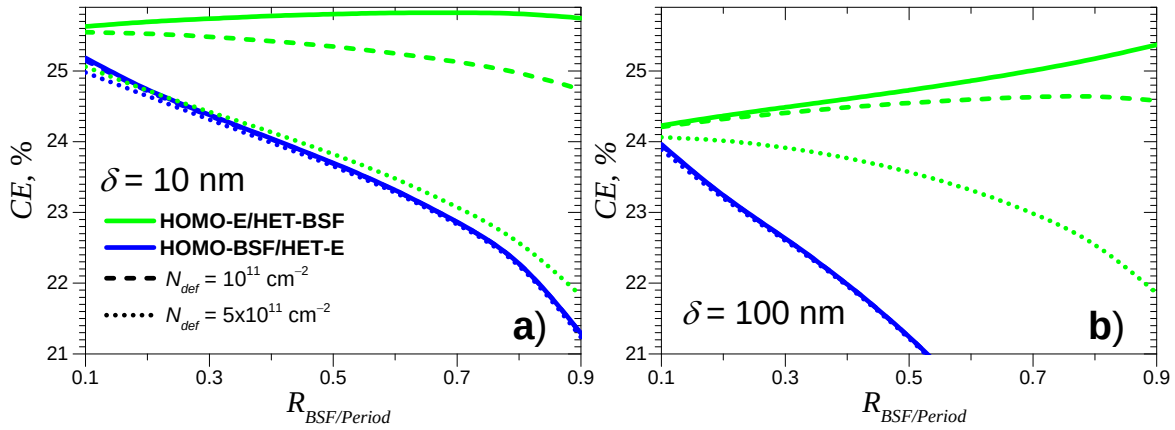

Fig. 4. Conversion efficiency calculated for Hybrid IBC solar cells as a function of $R_{BSF/Period}$ and for two different dopant penetration depths (δ): 10 nm (a) and 100 nm (b). For both cases *CE* was calculated including interface defects: ideal case without interface defects (solid lines), $N_{def} = 10^{11}$ cm^{-2} (dashed lines) and $N_{def} = 5\times10^{11}$ cm^{-2} (dotted lines).

4. Conclusions

One way to improve the solar energy conversion efficiency is to increase the open circuit voltage by increasing the concentration of dopants. However, this also leads to an increase of recombination of electron-hole pairs in the region of high doping. Thus, reducing the high doping area due to the doping depth is important for improving the conversion efficiency, as shown in this work. Furthermore, changing the doping depth is associated with a change of technology, namely the replacement of the diffusion method by ion implantation. This is more attractive, since the thermal diffusion typically occurs at a higher temperature, while the ion implantation process is a low temperature process. Moreover, the amount of dopants may be controlled more accurately in the case of ion implantation, in contrast to diffusion. Thus, the calculations performed in this study aimed to provide an insight into how the dopant penetration depth and the peak dopant concentration impact the IBC solar cells based on HOMO and hybrid structures. Notably, the simulations were performed for different values of $R_{BSF/Period}$, representing the ratio between the width of the BSF and the period of the back contact structure, and for different values of density of defects at the c-Si/a-Si:H heterointerface.

In the case of ideal interfaces it appears that the best solar performances are achieved by the Hybrid IBC solar cells for a very short dopant penetration depth ($\delta = 10$ nm) and a high peak dopant concentration (N_E, $N_{BSF} = 10^{21}$ cm^{-3}). In particular, a cell efficiency around 25-26% was calculated for $R_{BSF/Period} = 0.1$ which implies to reduce the width of the BSF with respect to the emitter. In case of a peak dopant concentration (N_E, N_{BSF}) below 10^{20} cm^{-3} a very shallow dopant penetration depth is not anymore required. For $\delta = 100$ nm the increase of the conversion efficiency requires an increase of the heterojunction width compared to the homojunction.

When including defects at the c-Si/a-Si:H interface it appears that HOMO-E/HET-BSF IBC structures are more affected, however, reducing the width of the HET-BSF ($R_{BSF/Period} = 0.1$) minimizes the *CE* losses. Lastly, the HOMO-BSF/HET-E IBC structures are not impacted by the interface defects implemented at the heterointerface for values up to 5×10^{11} cm^{-2}. This is because for such low interface defect densities the HOMO-BSF is always the limiting junction in terms of recombination. Solar cell efficiencies of 25% are achievable if the width of the BSF is greatly reduced and combined with highly doped homojunctions and shallow dopant penetration depths.

5. Acknowledgements

This work was supported by the project HERCULES that has received funding from the European Union's Seventh Programme for Research Technological Development and Demonstration under Grant agreement no. 608498 and the French Agence Nationale de la Recherche (ANR) under grant ANR-12-PRGE-0015 (project SMASH IBC2).

References

[1] Smith DD, Cousins P, Westerberg S, De Jesus-Tabajonda R, Aniero G, Shen YC. Toward the practical limits of silicon solar cells. IEEE J-PV 2014; 4:1465-1469.

[2] Franklin E et al. Fabrication and characterization of a 24.4% efficient IBC cell. Proc. 29th EU PVSEC, Amsterdam, The Netherlands, 2014, Prog. Photovolt: Res. Appl.; 2014. p.666-671.

[3] De Wolf S, Descoeudres A, Holman ZC, Ballif C. High-efficiency silicon heterojunction solar cells: a review. Green 2012; 2:7-24.

[4] Masuko K et al. Achievement of more than 25% conversion efficiency with crystalline silicon heterojunction solar cell. IEEE Journal of Photovoltaics 2014; 4:1433-1435.

[5] http://www.silvaco.com/products/tcad/ device_simulation/atlas/atlas.html

[6] Ghembaza H, Zerga A, Saïm R. Efficiency improvement of crystalline silicon solar cells by optimizing the doping profile of POCl3 diffusion. IJSTR 2014; 3:2277-8616.

[7] Gong C, Van Kerschaver E, Robbelein J, Janssens T, Posthuma N, Poortmans J, Mertens R. Screen-printed aluminum-alloyed p^+ emitter on high-efficiency n-type interdigitated back-contact silicon solar cells. IEEE Electron Device Letters. 2010; 31:576-578.

[8] Aleman M, Rosseel E, Van Wichelen K, Pawlak BJ, Janssens T, Dross F, Posthuma NE, Poortmans J. Ion implantation as a potential alternative for the formation of Front Surface Fields for IBC silicon solar cells. Proc. 35th Photovoltaic Specialists Conference (PVSC), June 2010, p.001291-0012945.

[9] Diouf D, Kleider JP, Desrues T, Ribeyron PJ. 2D simulations of interdigitated back contact heterojunction solar cells based on n-type crystalline silicon. Phys. Status Solidi C 2010; 7:1033-1036.